Journal of Medicinal Chemistry

Article

pubs.acs.org/jmc

Identification, Design and Biological Evaluation of Bisaryl Quinolones Targeting *Plasmodium falciparum* Type II NADH:Quinone Oxidoreductase (PfNDH2)

Chandrakala Pidathala,[†] Richard Amewu,[†] Bénédicte Pacorel,[†] Gemma L. Nixon,[‡] Peter Gibbons,[†] W. David Hong,[†] Suet C. Leung,[†] Neil G. Berry,*[,†] Raman Sharma,[‡] Paul A. Stocks,[‡] Abhishek Srivastava,[‡] Alison E. Shone,[‡] Sitthivut Charoensutthivarakul,[†] Lee Taylor,[†] Olivier Berger,[†] Alison Mbekeani,[‡] Alasdair Hill,[‡] Nicholas E. Fisher,[‡] Ashley J. Warman,[‡] Giancarlo A. Biagini,*[,‡] Stephen A. Ward,*[,‡] and Paul M. O'Neill*[,†]

[†]Department of Chemistry, University of Liverpool, Liverpool, L69 7ZD, U.K.

[‡]Liverpool School of Tropical Medicine, Pembroke Place, Liverpool, L3 5QA, U.K.

Supporting Information

ABSTRACT: A program was undertaken to identify hit compounds against NADH:ubiquinone oxidoreductase (PfNDH2), a dehydrogenase of the mitochondrial electron transport chain of the malaria parasite *Plasmodium falciparum*. PfNDH2 has only one known inhibitor, hydroxy-2-dodecyl-4-(1H)-quinolone (HDQ), and this was used along with a range of chemoinformatics methods in the rational selection of 17 000 compounds for high-throughput screening. Twelve distinct chemotypes were identified and briefly examined leading to the selection of the quinolone core as the key target for structure−activity relationship (SAR) development. Extensive structural exploration led to the selection of 2-bisaryl 3-methyl quinolones as a series for further biological evaluation. The lead compound within this series 7-chloro-3-methyl-2-(4-(4-(trifluoromethoxy)benzyl)phenyl)quinolin-4(1H)-one (CK-2-68) has antimalarial activity against the 3D7 strain of *P. falciparum* of 36 nM, is selective for PfNDH2 over other respiratory enzymes (inhibitory IC_{50} against PfNDH2 of 16 nM), and demonstrates low cytotoxicity and high metabolic stability in the presence of human liver microsomes. This lead compound and its phosphate pro-drug have potent in vivo antimalarial activity after oral administration, consistent with the target product profile of a drug for the treatment of uncomplicated malaria. Other quinolones presented (e.g., **6d**, **6f**, **14e**) have the capacity to inhibit both PfNDH2 and *P. falciparum* cytochrome bc_1, and studies to determine the potential advantage of this dual-targeting effect are in progress.

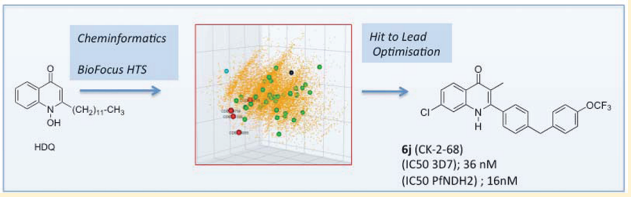

INTRODUCTION

Drug resistance to currently deployed, established antimalarials such as chloroquine is driving the rise in global mortality due to malaria.[1] Malaria is responsible for roughly one million deaths annually,[2] and as such novel inhibitors active against new parasite targets are urgently required in order to sustain and develop treatments against malaria.[3] To this end, a program was undertaken to identify hit compounds active against the electron transport chain (ETC) of *Plasmodium falciparum* and specifically against NADH:ubiquinone oxidoreductase (PfNDH2).

PfNDH2 is a single subunit 52 kDa enzyme involved in the redox reaction of NADH oxidation with subsequent quinol production.[4] Localized in the mitochondrion, PfNDH2 is a principal elctron donor to the ETC, linking fermentative metabolism to the generation of mitochondrial electrochemical membrane potential ($\Delta\psi m$), an essential function for parasite viability (Figure 1).[4] Targeting the electron transport chain of the mitochondrion is a proven drug target as demonstrated by the drug atovaquone, targeting the cytochrome bc_1 complex.[5]

In order to identify hit compounds, we employed a range of ligand-based chemoinformatics methods in the rational selection of approximately 17 000 compounds that were predicted to possess activity against PfNDH2. The chemoinformatics approach were initiated from the identity of only one inhibitor of the target, hydroxy-2-dodecyl-4-(1H)-quinolone (HDQ)[6] and used molecular fingerprints,[7] turbo similarity,[8] principal components analysis, Bayesian modeling,[9] and bioisosteric[10] replacement in order to select compounds for high-throughput screening (HTS). The compounds were selected from a commercial library of ~750 000 compounds (Biofocus DPI) and were predicted to possess favorable absorption, distribution, metabolism, excretion, and toxicity (ADMET) characteristics.[11] The selected compounds were subject to a sequential high-throughput screening methodology using an in vitro assay against recombinant PfNDH2 as described previously.[6] Hit confirmation and potency determination

Received: September 6, 2011
Published: February 24, 2012

dx.doi.org/10.1021/jm201179h | *J. Med. Chem.* 2012, 55, 1831−1843

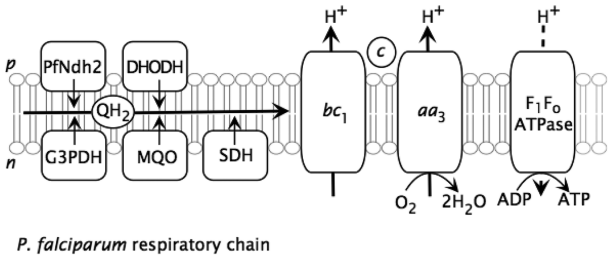

Figure 1. Mitochondrial electron transfer chain and the role of PfNDH2 and bc_1. Schematic representation of the respiratory chains of *P. falciparum* and *M. tuberculosis*. The chain components are (i) *P. falciparum*: PfNDH2 – type II NADH:quinone oxidoreductase, DHODH – dihydroorotate dehydrogenase, G3PDH – glycerol-3-phosphate dehydrogenase, MQO – malate:quinone oxidoreductase, SDH – succinate dehydrogenase, bc_1 – cytochrome bc_1 complex, *c* – cytochrome *c*, aa_3 – cytochrome *c* oxidase and the F_1F_o-ATPase (Complex V).

revealed over 40 compounds with IC_{50} values ranging from below 50 nM to 40 μM. Analysis of these hits revealed that only two of the compounds were selected by more than one chemoinformatic method, justifying the use of several virtual screening approaches. Seven distinct chemotypes were identified from the hit compounds and were thus primed for development as new agents against malaria (see Supporting Information). All 12 distinct chemotypes were briefly examined and key compounds were synthesized, and this led to the selection of the quinolone core as one of the main target chemotypes for structure–activity relationship (SAR) development due to its HDQ-like structure (Figure 2).

Quinolones identified from the HTS were not considered appropriate for further optimization (see CDE204758 and CDE264055) but given the high potency of hit CDE021056, versus PfNDH2, we selected 2-substituted monoaryl quinolones as a core template with potential for SAR development (Note that several low micromolar saturated quinolones, e.g., CDD038715, were identified in this screen). The rationale for selection of the 2-aryl quinolone pharmacophore was to introduce additional lipophilicity in a region where HDQ contains the flexible aliphatic side chain. Subsequently, further extension of the side chain was performed, so it is more HDQ-like, while incorporating functionality to impart metabolic stability within the analogue series, and this approach led to eventual identification of early lead compounds for this series. In terms of SAR, the nature of the group at 3-position, the electronic/steric effect of substituents placed at the 5, 6, and 7 positions, the presence of a nitrogen in the A ring of the quinolone core, and changing from NH to NOH (as in HDQ) were all examined (Figure 2).

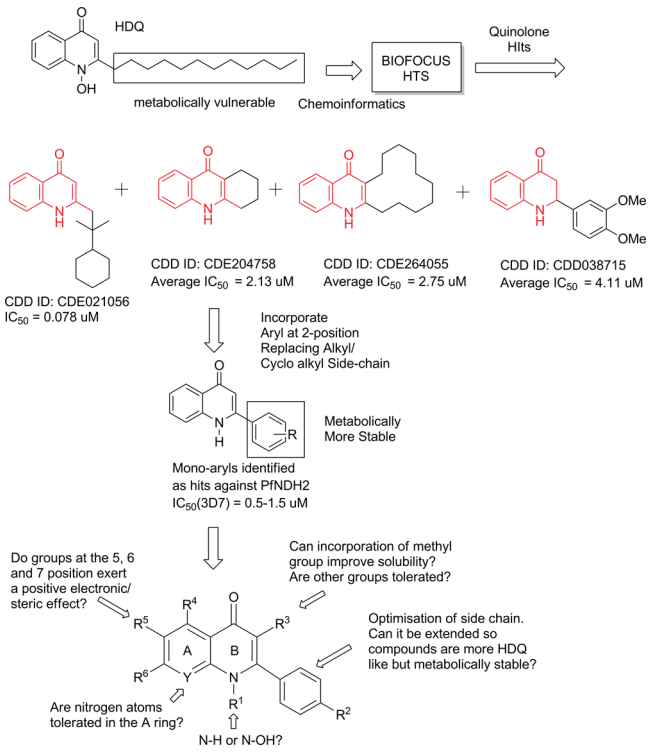

Figure 2. Mono 2-aryl quinolones emerging from quinolone hits identified in high-throughput screen and initial SAR performed on template.

RESULTS

Having identified mono aryl quinolones as hits against the target PfNDH2 (ca. 50–250 nM, e.g., **14a** and **15a**) with moderate activity in the whole cell phenotypic screen, our efforts were initially concentrated on the synthesis of a small number of additional analogues to see if activity could be improved further. The first structural alteration was to introduce a methyl substituent at the three position (e.g., **6a**); this manipulation twists the 2-aryl side-chain, altering the torsion angle (Figure 3) leading to a subsequent reduction in aggregation.

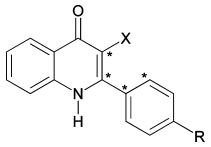

Figure 3. The torsion angle that best represents the planarity of the 2-aryl group with respect to the quinolone core.

Aggregation via π-stacking of aromatic ring systems leads to higher melting points,[12] which has been shown to be closely related to solubility.[13] Molecular modeling was performed in order to analyze the relationship between melting point and the conformational effect of introducing a methyl or chloro group at the three position of the quinolone. Monte Carlo simulations were performed in order to sample the thermally accessible conformations and calculate the Boltzmann weighted average torsion angle that best described the planarity of the 2-position aryl ring with respect to the quinolone ring (see Figure 3 for torsional angle and Supporting Information for computational details).

The melting point and computed Boltzmann weighted average torsion angle were examined for four pairs of compounds: **6a** and **14a**, **6b** and **14a**, **14c** and **15a**, and finally **6d** and **14e**; compounds within a pair are close analogues of each other with one compound incorporating a hydrogen substituent at the 3-position and the other either a methyl or chloro group. Higher melting points within a pair were found to correlate with a hydrogen substituent at the 3-position; conversely, lower melting points correlated with the presence of more bulky methyl or chloro groups. Hydrogen substituted compounds were found to have lower computed thermally accessible torsional angles than their methyl-substituted counterparts, as exemplified by compounds **6a** and **14a** (Figure 4,

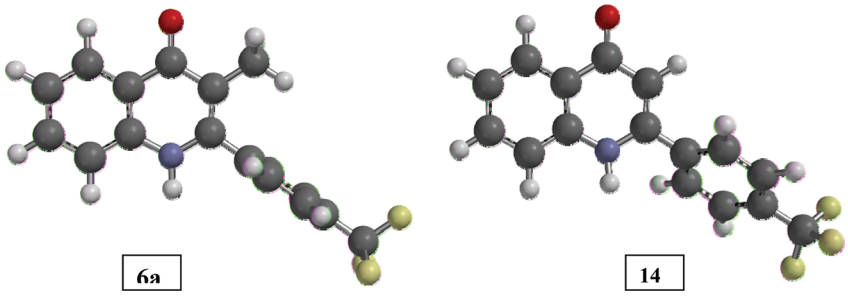

Compound	3-X	Melting Point/°C	Boltzmann Weighted Average Torsional Angle/°
6a	Me	289	87.61
14a	H	340	60.33

Figure 4. Lowest energy conformations for compounds **6a** and **14a**. Carbon, hydrogen, nitrogen, oxygen, and fluorine atoms are depicted in dark gray, off-white, blue, red, and pale-yellow respectively. The accompanying table shows the corresponding melting points and computed Boltzmann weighted average torsional angles. Images were produced in the Spartan '08 Version 1.0.0 (Wavefunction Inc., Irvine, CA, USA).

see Supporting Information for information for all pairs of compounds). This analysis supports the hypothesis that the solubility is related to the planarity/π-stacking propensity of 2-aryl substituted quinolones.

Other structural modifications investigated for the mono aryl series were the presence of a nitrogen within the A ring of the quinolone core, altering the phenyl substituent and using H or Cl at the 3-position. From preliminary testing against the 3D7 strain of *P. falciparum*, it rapidly became apparent that activities below 500 nM versus the 3D7 strain could not be achieved. The chemistry employed to synthesize these compounds and their structures are covered in Schemes 1−4 and Tables 1−4 which will be described in detail for the subsequent bisaryl compounds.

Being cognizant of the HDQ inhibitory activity against PfNDH2, compounds were designed with an extended side chain. In order to avoid the metabolically unstable HDQ side chain, a bisaryl group was chosen to mimic this side chain but maintain metabolic stability. The first series of compounds contains a methyl group at the 3-position (Scheme 1 and Table 1).

Scheme 1. Synthesis of Quinolones 6a−w

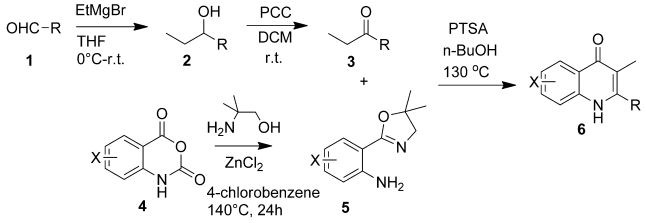

Bisaryl compounds with a CH_2 and O linker were investigated with the nature of the terminal phenyl substituent being varied along with the position of the linker. The presence of additional substituents around the A ring of the quinolone core was also looked at in detail.

The synthesis of these compounds was achieved in 4−6 steps from commercially available, inexpensive starting materials. Aldehyde **1** was utilized in a Grignard reaction to give alcohol **2** in 70−99% yields. Where aldehyde **1** was not commercially available, the aldehydes were synthesized in house (see Supporting Information). Alcohol **2** was oxidized using PCC to give ketone **3** in 80−99% yields. Oxazoline **5** was prepared from the respective isatoic anhydride **4** in yields of 40−60%. In the majority of compounds, the isatoic anhydrides were commercially available; when this was not the case they were synthesized (see Supporting Information). Reaction of oxazoline **5** with ketone **3** in the presence of PTSA gave the desired quinolones **6a−w** in 20−85% yields.[14]

A selection of methoxy quinolones **6n−p** were then demethylated using BBr_3 to give hydroxy quinolones **7a−c** in 51−69% yields. **7c** was then acetylated using triethylamine and acetyl chloride to give quinolone **8** in 70% yield (Scheme 2).

Where yields of 3-methyl quinolones were very low in the final step, the methodology depicted in Scheme 3 was employed. This route was also the highest yielding for compounds containing a nitrogen within the A ring of the quinolone core. Ketone **3** was converted to dimethoxy acetal **9** in 40−90% yield using trimethyl orthoformate and PTSA. Reaction of diacetal **9** with various anthranilic acids **10** by refluxing in Dowtherm A gave quinolones **11a−h** in 43−66% yields (Scheme 3 and Table 2).

Analogues with a hydrogen at the 3-position were also synthesized (Scheme 4 and Table 3). In this case ketone **3** was reacted with diazo ethyl malonate to give diketylester **12** in 58−68% yield. Reaction with a variety of anilines gave amine **13** in 52−78% yield. Heating amine **13** in Dowtherm A gave the desired quinolones **14a−k** in 48−70% yield. Crystals of quinolone **14e** were grown and its structure was confirmed by X-ray crystallography (see Figure 5, CCDC 833920). The effect of a hydroxyl group both in the A ring of the quinolone core and at the terminal end of the side chain was explored. To this end it was necessary to treat 7-OMe quinolone **14h** with BBr_3 to give 7-OH quinolone **14l** in 60% yield. Treatment of **14k** containing a side chain with a terminal methyl ester with LAH gave **14m** with a terminal methyl alcohol in 78% yield.

It has been shown from GSK's pyridone series that the presence of a chlorine at the 3-position was well tolerated.[15] With this in mind a selection of the 3-H compounds were treated with sodium dichloroisocyanurate and sodium hydroxide to give 3-chloro quinolones **15a−c** in 53−64% yields.

While we believe the 2-bisaryl 3-methyl quinolones to be optimal for antimalarial activity and PfNDH2 selectivity, it was a logical progression to investigate how interchanging the two

dx.doi.org/10.1021/jm201179h | *J. Med. Chem.* 2012, 55, 1831−1843

Table 1. Yields for the Synthesis of Compounds 6a−w

compound	R	X	% yield **2**	% yield **3**	% yield **5**	% yield **6**
6a	-Ph*p*CF_3	H			45	32
6b	-Ph*p*OCF_3	H			45	32
6c	-Ph*p*CH_2Ph	H	72	94	45	42
6d	-Ph*p*CH_2Ph*p*OCF_3	H	99	99	45	42
6e	-Ph*m*CH_2Ph*p*OCF_3	H	78	82	45	30
6f	-Ph*p*CH_2Ph*p*F	H	97	97	45	20
6g	-Ph*p*CH_2Ph*p*OMe	H	71	90	45	32
6h	-Ph*p*CH_2Ph*p*OCF_3	6-CF_3	99	99	51	52
6i	-Ph*p*CH_2Ph*p*OCF_3	7-CF_3	99	99	55	24
6j (CK-2-68)	-Ph*p*CH_2Ph*p*OCF_3	7-Cl	99	99	58	30
6k	-Ph*p*CH_2Ph*p*OCF_3	6-Cl, 7-F	99	99	41	34
6l	-Ph*p*CH_2Ph*p*OCF_3	6-F, 7-Cl	99	99	30	27
6m	-Ph*p*CH_2Ph*p*OCF_3	5-OMe	99	99	98	8
6n	-Ph*p*CH_2Ph*p*OCF_3	6-OMe	99	99	48	28
6o	-Ph*p*CH_2Ph*p*OCF_3	7-OMe	99	99	21	29
6p	-Ph*p*CH_2Ph*p*OCF_3	8-OMe	99	99	30	27
6q	-Ph*m*CH_2Ph*p*OCF_3	6-Cl	78	82	47	20
6r	-Ph*m*CH_2Ph*p*OCF_3	7-Cl	78	82	58	30
6s	-Ph*p*CH_2Ph*p*F	7-Cl	97	97	58	16
6t	-Ph2F*p*CH_2Ph*p*OCF_3	7-Cl	88	88	58	35
6u	-Ph*p*OPh*p*OCF_3	H		63[a]	45	28
6v	-Ph*p*OPh*p*OCF_3	7-Cl		63[a]	58	32
6w	-Ph*p*OPh*p*Cl	H	84	91	45	8.5

[a]Alternative route please see Supporting Information.

Scheme 2. Synthesis of Quinolones 7a−c and 8

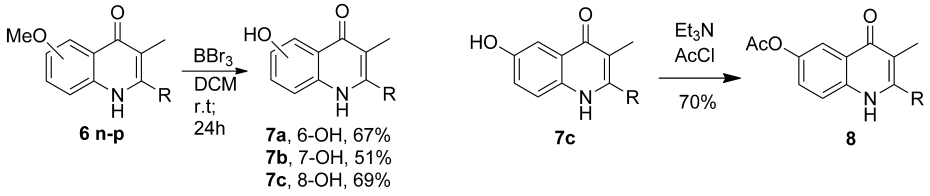

Scheme 3. Synthesis of Quinolones 11a−h

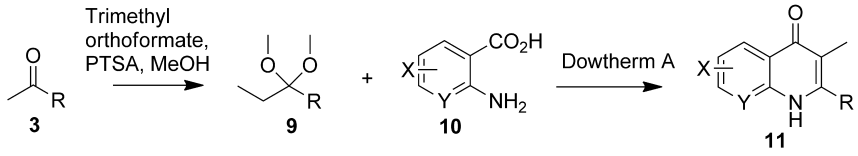

Table 2. Yields for the Synthesis of Compounds 11a−h

compound	R	X	Y	% yield **9**	% yield **11**
11a	-Ph*p*CF_3	H	N	45	46
11b	-Ph*p*OCF_3	H	N	89	56
11c	-Ph*p*OMe	H	N	58	43
11d	-Ph*p*Br	H	N	55	66
11e	-Ph*p*CH_2Ph*p*OCF_3	H	N	89	44
11f	-Ph*p*CH_2Ph*p*OCF_3	7-F	CH	89	44
11g	-Ph*p*CH_2Ph*p*OCF_3	6-F, 7-F	CH	89	39
11h	-Ph*p*CH_2Ph*p*F	H	N	76	42

substituents would influence both activity and selectivity. The first compounds synthesized were the 3-aryl variants of **6d** and **6u**. Ketone **16** was reacted with oxazoline **17** to give the 3-monoaryl quinolone **18** in 27% yield. Reaction of quinolone **18** with the boronic ester **19** gave the desired 3-bisaryl quinolone **20** in 89% yield (see Figure 6). For the **6u** variant quinolone **18** was reacted with phenol **21** in 30% yield to give the 3-bisaryl quinolone **22** with an oxygen linked side chain. The synthesis of hydroxymethyl quinolone **25** was undertaken to see if a hydroxymethyl group was tolerated in the molecule[15] in order to provide a handle for the synthesis of appropriate pro-drugs such as phosphates[16] or carbamates.[17] Reaction of quinolone **22** with ethyl chloroformate gave ester **23** in 70% yield, and subsequent reaction with selenium dioxide in dioxane gave a 98% yield of aldehyde **24**. This was followed by conversion to the alcohol **25** in 69% yield. Synthesis of 2-H, 3-bisaryl quinolone **29** was achieved by carrying out a Suzuki reaction on chloro, bromo quinoline **26** in 45% yield. A further Suzuki reaction was then undertaken to give chloro quinoline **28** in 50% yield. Conversion to quinolone **29** was achieved using formic acid in 94% yield.

Further investigation into the nature of the group tolerated at the 3-position was carried out. Quinolones **32a−c** containing an ethyl ester at the 3-position were synthesized by reacting

dx.doi.org/10.1021/jm201179h | J. Med. Chem. 2012, 55, 1831−1843

Scheme 4. Synthesis of Quinolones 14a−m

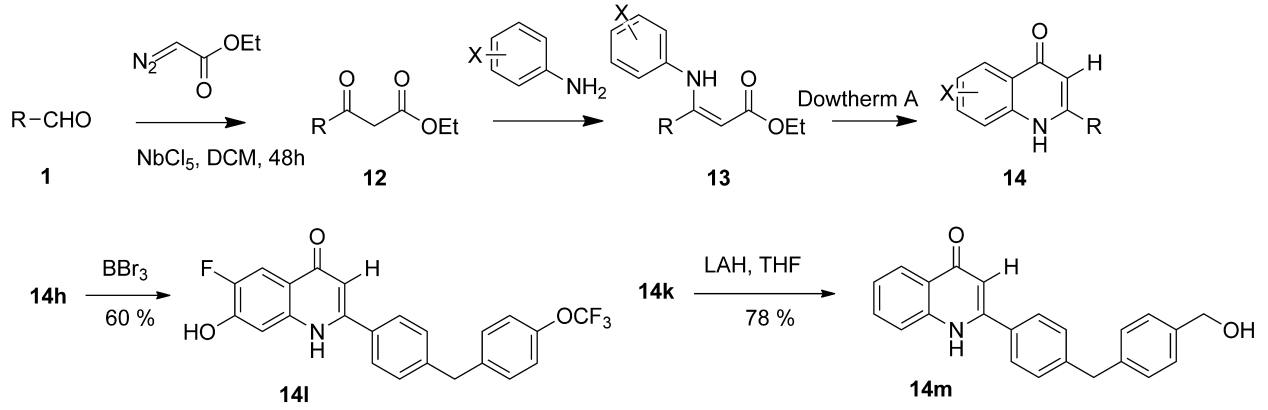

Table 3. Yields of Quinolones 14a−k

Compound	R	X	% Yield **12**	% Yield **13**	% Yield **14**
14a	-Ph*p*CF_3	H	58	72	70
14b	-Ph*p*OCF_3	H	64	62	68
14c	-Ph*p*OMe	H	61	66	70
14d	-Ph*p*OH	H	60	68	58
14e	-Ph*p*CH_2Ph*p*OCF_3	H	68	78	70
14f	-Ph*p*CH_2Ph*p*OCF_3	6-F, 7-F	68	64	67
14g	-Ph*p*CH_2Ph*p*OCF_3	6-Cl, 7-Cl	68	66	72
14h	-Ph*p*CH_2Ph*p*OCF_3	6-F, 7-OMe	68	72	56
14i	-Ph*p*CH_2Ph*p*OCF_3	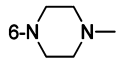	68	56	56
14j	-Ph*p*CH_2Ph*p*OCF_3	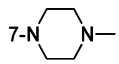	68	52	48
14k	-Ph*p*CH_2Ph*p*CO_2Me	H	49	72	63

Table 4. Yields for the Synthesis of Compounds 15a−c

compound	R	% yield **15**
15a	OCF_3	60
15b	OMe	53
15c	CH_2Ph*p*OCF_3	64

isatoic anhydride **30** with *β*-keto ester **31** in the presence of NaH and DMF in 30−35% yield (see Figure 7). The presence of a methyl alcohol at the 3-position could then be achieved using LAH to convert the esters to 3-methyl alcohol quinolones **33a** and **33b** in 46% and 48% yields.

As there are several examples of naturally occurring 1-hydroxy-4(1*H*)-quinolones that are known inhibitors of respiratory and photosynthetic electron transport chains,[18] it was logical to explore the effect of an N−OH variant of our template on antimalarial activity and PfNDH2 activity. Synthesis of the N−OH compounds was achieved by reacting the quinolone with ethyl chloroformate to give carbonate **34** in

dx.doi.org/10.1021/jm201179h | *J. Med. Chem.* 2012, 55, 1831−1843

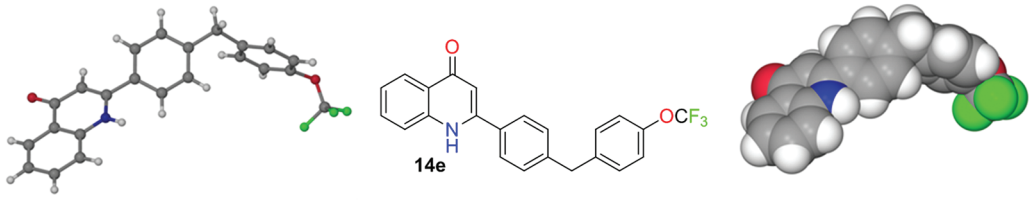

Figure 5. X-ray crystal structure of quinolone **14e**.

Scheme 5. Synthesis of Chloro Quinolones 15a–c

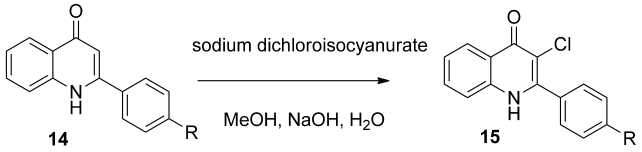

60–99% yield. Synthesis of the *N*-hydroxy analogues via the carbonate intermediate was advantageous as the carbonates themselves are possible pro-drugs and so subsequently were also tested for antimalarial activity. This was then oxidized using *m*-CPBA to give the *N*-oxide **35** which was used crude in the final step. Reaction with KOH gives the desired *N*-hydroxy compound **36** in 80–98% yield (Scheme 8).[19]

Optimization of the side chain to improve solubility and drug delivery is key to the successful development of these hits, and there are several strategies that we have adopted to date. Further modifications to the side chain have included extending the terminal group using an oxy-linked alkyl morpholine to provide the opportunity for developing molecules that can be formulated as salts. This type of approach has been applied in the development of kinase inhibitors where incorporation of cyclic amine groups such as morpholine has transformed highly insoluble compounds into candidates with excellent drug-like properties.[20] To incorporate the oxyl-linked morpholine side chain bisaryl aldehyde **37** was converted to the ethyl ketone **39** using chemistry described previously. BBr_3 was then used to demethylate **39** to give alcohol **40** in 50–70% yields. Addition of the ethyl morpholine subunit was achieved using potassium carbonate to give side chain **41** in 86% yields. Reaction with oxazoline **5a** in the presence of triflic acid gave quinolones **42 a–c** in 30–55% yields (Scheme 9).

While our primary focus was to use medicinal chemistry manipulation of the core template to maximize solubility and activity, pro-drug approaches were also briefly examined. Pro-drugs have been successfully adopted by GSK in their antimalarial pyridone (GSK932121) program. Impressive in vivo antimalarial activity and exposure profiles have been

Scheme 6. Synthesis of 3-Aryl Quinolones 20, 22, 25, and 29

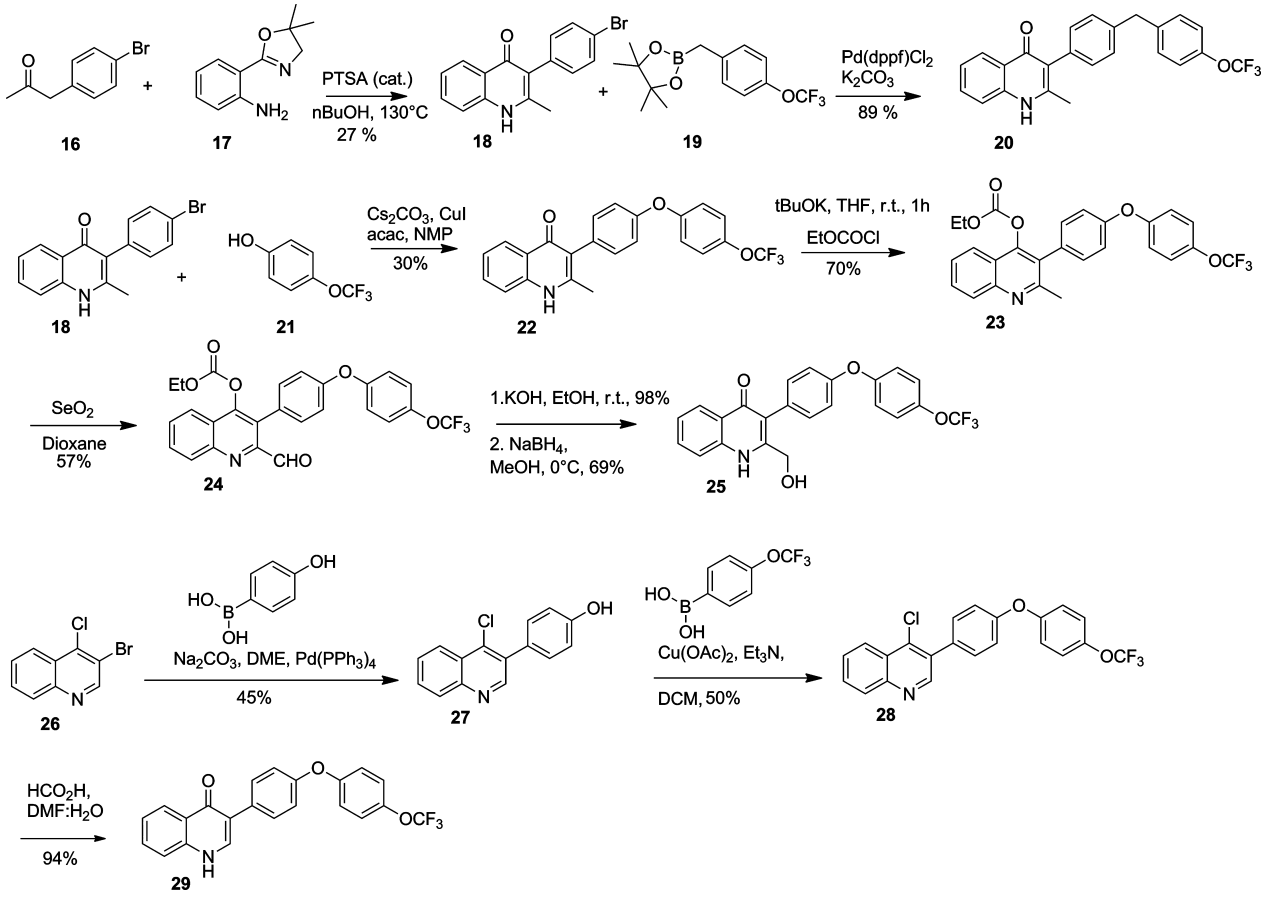

dx.doi.org/10.1021/jm201179h | *J. Med. Chem.* 2012, 55, 1831–1843

Scheme 7. Synthesis of 3-Ethyl Ester and 3-Hydroxymethyl Quinolones 32a–c and 33a,b

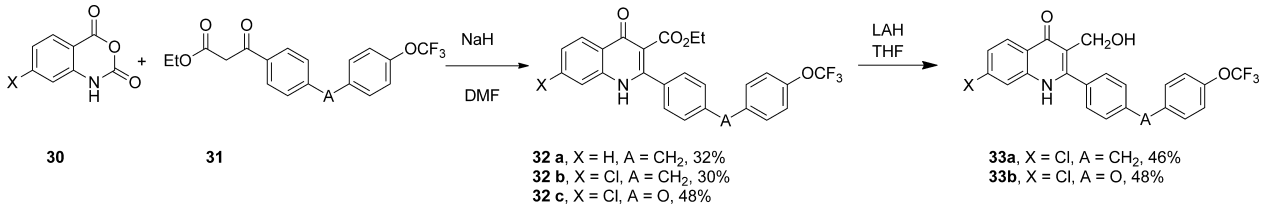

Scheme 8. Synthesis of N–OH Quinolones 36a–e

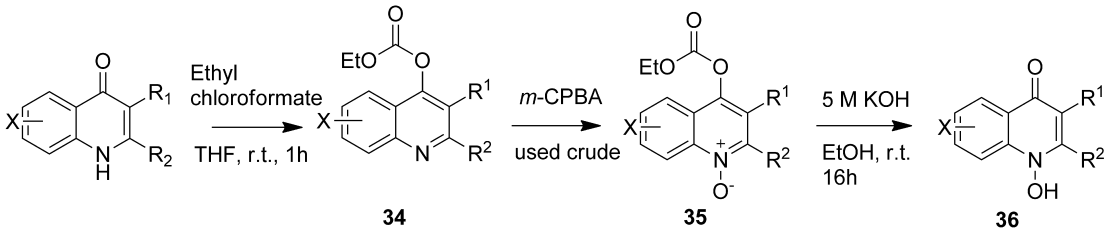

Table 5. Yields of Carbamates 34a–d and *N*-Hydroxy Quinolones 36a–d

compound	R^1	R^2	X	% yield **34**	% yield **36**
36a	Me	-Ph*p*CH_2Ph*p*OCF_3	H	98	98
36b	Me	-Ph*p*CH_2Ph*p*OCF_3	7-Cl	67	80
36c	-Ph*p*CH_2Ph*p*OCF_3	Me	H	99	91
36d	H	-Ph*p*CH_2Ph*p*OCF_3	H	88	98
36e	Me	-Ph*p*OPh*p*OCF_3	H	60	83

Scheme 9. Synthesis of Extended Side Chain Ethoxy Morpholine Quinolones 42a–c

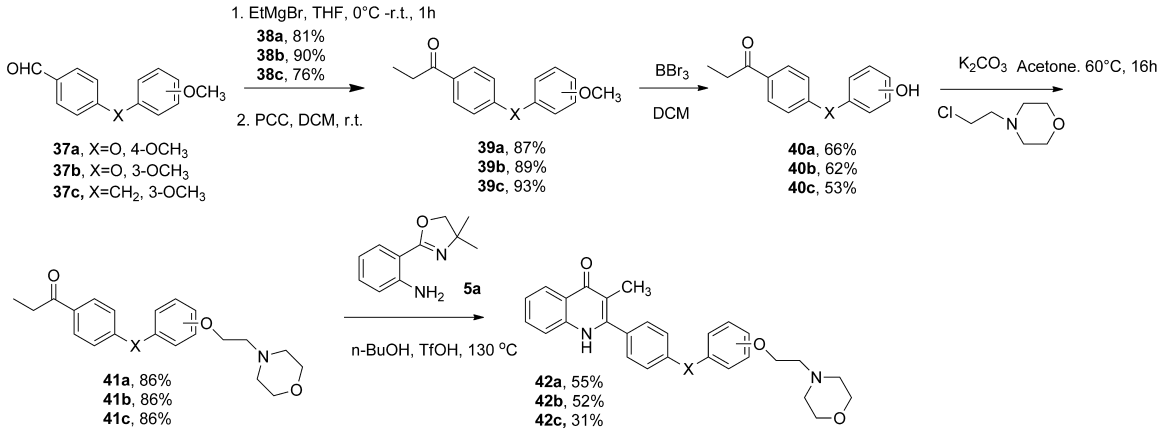

achieved with pyridone-based phosphate pro-drugs.[16] Phosphate ester pro-drugs are highly ionized at physiological pH, highly soluble in water, are chemically stable and enzymatic cleavage at the gut wall by membrane-bound alkaline phosphatases produces high concentrations of the parent drug in the systemic circulation. Phosphate pro-drugs have also been successfully developed for the 2-arylquinolone series of anticancer agents developed by Chou et al. where CHM-1-PNa was developed as a novel water-soluble drug candidate (Figure 6).[21] Morpholine carbamate pro-drugs were also investigated.[17]

Compound **6j** was used for the basis of our pro-drug work as it exhibited good in vitro antimalarial activity and selectivity against PfNDH2 (see below). Quinolone **6j** was reacted with tetrabenzyl pyrophosphate in the presence of NaH to give the phosphonate ester **43** in 87% yield. Hydrogenation using Pd/C gave phosphate pro-drug **44** in 80% yield (Scheme 10).

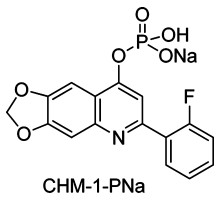

Figure 6. Phosphate pro-drug of anticancer drug CHM-1-PNa.

Morpholine carbamate pro-drug **45** was made by reacting quinolone **6j** with morpholine carbonyl chloride in the presence of potassium *tert*-butoxide to give the pro-drug in 66% yield (Scheme 11).

dx.doi.org/10.1021/jm201179h | *J. Med. Chem.* 2012, 55, 1831–1843

Scheme 10. Synthesis of Phosphate Pro-Drug 44

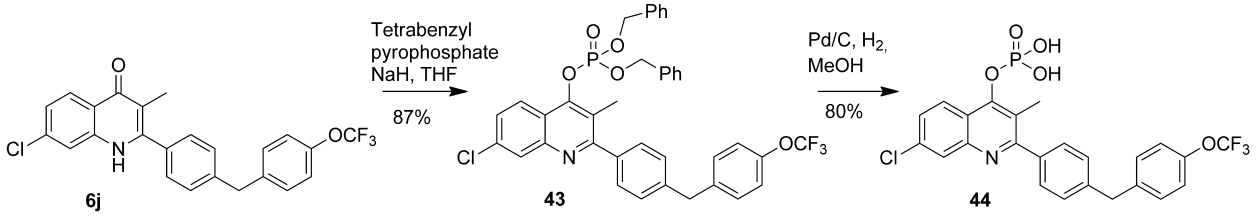

Scheme 11. Synthesis of Morpholine Pro-Drug 45

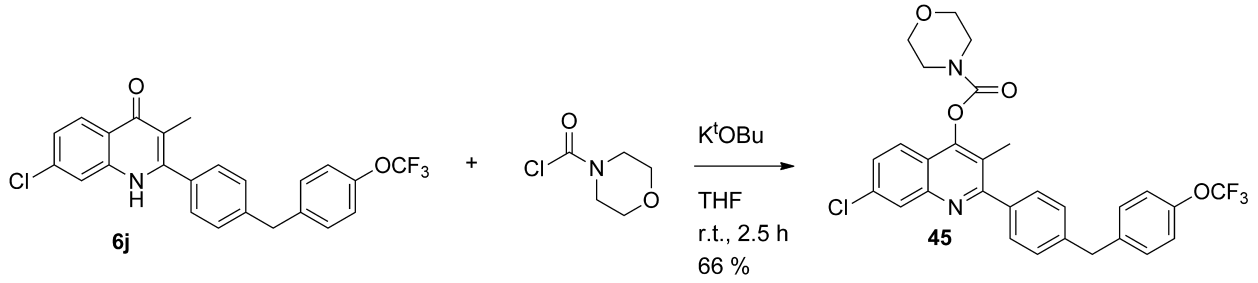

Table 6. In Vitro Antimalarial Activities of Monocyclic Quinolones versus 3D7 *P. falciparum*

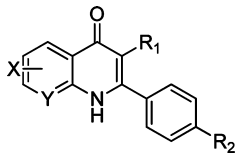

compound	X	Y	R^1	R^2	IC_{50} (nM) 3D7 ± SD/(IC_{50} (nM) $PfNDH_2$)
6a	H	CH	Me	CF_3	752 ± 7.8/(88.5)
6b	H	CH	Me	OCF_3	>1000
11a	H	N	Me	CF_3	>1000
11b	H	N	Me	OCF_3	>1000
11c	H	N	Me	OMe	>1000
11d	H	N	Me	Br	>1000
14a	H	CH	H	CF_3	579 ± 120/(52.90)
14b	H	CH	H	OCF_3	675 ± 80/(47.9)
14c	H	CH	H	OMe	>1000
14d	H	CH	H	OH	>1000
15a	H	CH	Cl	OCF_3	513 ± 134/(253)
15b	H	CH	Cl	OMe	560 ± 110/(1670)

Further strategies including the use of polar heterocycles in the side chain, use of other protonatable groups within the side chain, extending the terminal group using polar heterocycles, and the placement of a polar group centrally in the side chain with a lipophilic group at the terminal end are covered in the subsequent paper.

Antimalarial Activity. Tables 6, 7, and 8 show the antimalarial activity of all quinolones synthesized against the 3D7 strain of *P. falciparum*. Table 6 shows activity for monoaryl analogues and while activity of these compounds is generally poor, a few key points can be taken from these results in terms of SAR. In the case of monocyclic compounds, there is a definite trend toward better activity when CF_3 groups are present in the side chain and when a chlorine atom is present at the 3-position. Nitrogen within the A ring of the quinolone core results in reduced activity.

Table 7 shows the antimalarial activities of quinolones **6c−w**, **11e−h**, **14e−14m**, and **15c**. Clear trends are seen in the nature of the A ring substituent X. Generally the presence of Cl and F on the A ring is well tolerated and often enhances activity as seen when comparing **6d** (117 nM) to **6j** (36 nM), **6k** (70 nM), and **6l** (38 nM). Larger A ring substituents such as CF_3 as in the case of **6h** (654 nM) and **6i** (212 nM) and piperazine (**14i**, 430 nM and **14j**, 443 nM) are less well tolerated with a 10-fold drop in activity seen. The presence of an OMe group on the A ring is tolerated with substitution at the 7-position greatly enhancing activity. **6o** has activity of 8 nM activity whereas all other regioisomeric OMe compounds exhibit antimalarial activity of >350 nM (**6m**, **n** and **p**). Substitution at the 7-position is also favorable when looking at OH substitution (**7b**, 139 nM versus **7a**, 465 nM and **7c**, 819 nM). Nitrogens within the A ring are also not tolerated well as seen with **11e** (407 nM) and **11h** (506 nM). Of the three substituents examined at the 3-position all are well-tolerated. A hydrogen at the 3-position (R^1) does seem to offer a small advantage in terms of activity when comparing **14e** (48 nM) to **6d** (117 nM) and **14f** (16 nM) to **11g** (24 nM); however, this small increase in activity is far outweighed by the decrease seen in solubility. When comparing **15c** (19 nM) with **6d** (117 nM) the presence of a chlorine atom greatly enhances

dx.doi.org/10.1021/jm201179h | *J. Med. Chem.* 2012, 55, 1831−1843

Table 7. In Vitro Antimalarial Activities of Bicyclic Quinolones versus 3D7 *P. falciparum**

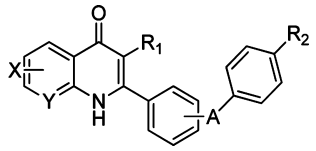

Compound	X	Y	A	R^1	R^2	IC_{50} (nM) 3D7 ± SD/ (IC_{50} (nM) $PfNDH_2$)
6c	H	CH	*p*CH_2	Me	H	107 ± 14 / (27.4)
6d	H	CH	*p*CH_2	Me	OCF_3	117 ± 27 / (16)
6e	H	CH	*m*CH_2	Me	OCF_3	26 ± 2 / (50)
6f	H	CH	*p*CH_2	Me	F	83 ± 9 / (<1)
6g	H	CH	*p*CH_2	Me	OMe	35 ± 7 / (113)
6h	6-CF_3	CH	*p*CH_2	Me	OCF_3	654 ± 138
6i	7-CF_3	CH	*p*CH_2	Me	OCF_3	212 ± 51
6j	7-Cl	CH	*p*CH_2	Me	OCF_3	36 ± 5 / (16)
6k	6-Cl, 7-F	CH	*p*CH_2	Me	OCF_3	70 ± 15
6l	6-F, 7-Cl	CH	*p*CH_2	Me	OCF_3	38 ± 5
6m	5-OMe	CH	*p*CH_2	Me	OCF_3	664 ± 80
6n	6-OMe	CH	*p*CH_2	Me	OCF_3	465 ± 39
6o	7-OMe	CH	*p*CH_2	Me	OCF_3	8 ± 2
6p	8-OMe	CH	*p*CH_2	Me	OCF_3	381 ± 45
6q	6-Cl	CH	*m*CH_2	Me	OCF_3	8.4 ± 0.4
6r	7-Cl	CH	*m*CH_2	Me	OCF_3	34 ± 6
6s	7-Cl	CH	*m*CH_2	Me	F	105 ± 15 / (196)
6t*	7-Cl	CH	*p*CH_2	Me	OCF_3	30 ± 10
6u	H	CH	*p*O	Me	OCF_3	26 ± 1 / (9.9)
6v	7-Cl	CH	*p*O	Me	OCF_3	73 ± 19 (32.2)
6w	H	CH	*p*O	Me	Cl	230 ± 43 (36)
7a	6-OH		*p*CH_2	Me	OCF_3	465 ± 39
7b	7-OH		*p*CH_2	Me	OCF_3	139 ± 20
7c	8-OH		*p*CH_2	Me	OCF_3	819 ± 50
8	6-OAc		*p*CH_2	Me	OCF_3	408 ± 140
11e	H	N	*p*CH_2	Me	OCF_3	407 ± 39 / (97)
11f	7-F	CH	*p*CH_2	Me	OCF_3	69 ± 11 / (12.1)
11g	6-F, 7-F	CH	*p*CH_2	Me	OCF_3	24 ± 6 / (30.9)
11h	H	N	*p*CH_2	Me	F	506 ± 65
14e	H	CH	*p*CH_2	H	OCF_3	48 ± 7 / (6.2)
14f	6-F, 7-F	CH	*p*CH_2	H	OCF_3	16 ± 4
14g	6-Cl, 7-Cl	CH	*p*CH_2	H	OCF_3	28 ± 9 / (173)
14h	6-F, 7-OMe	CH	*p*CH_2	H	OCF_3	39 ± 9
14i		CH	*p*CH_2	H	OCF_3	430 ± 80
14j		CH	*p*CH_2	H	OCF_3	443 ± 59
14k	H	CH	*p*CH_2	H	CO_2Me	272 ± 44 / (19)
14l	6-F, 7-OH	CH	*p*CH_2	H	OCF_3	>1000
14m	H	CH	*p*CH_2	H	CH_2OH	>1000
15c	H	CH	*p*CH_2	Cl	OCF_3	19 ± 6 / (137)

*First aromatic ring attached to quinolone core has a 2-F substituent. [a]P*fbc*$_1$ IC_{50} data (nM): **6d** = 37.5, **6e** = 219, **6f** = 25.5, **6j** = 9800, **14e** = 13.9.

activity, and this observation will be employed in future lead optimization campaigns in this area.

Looking in detail at the side chain, linker A variants para-CH_2, meta-CH_2, and para-O are all well tolerated with activity effects being determined by other areas of the molecule. The effect of the side chain terminal substituent is highly dependent on other functionality within the molecule, but as a general rule OCF_3 is the optimal terminal group as demonstrated by the comparison of **6r** (34 nM) to **6s** (105 nM) and **6u** (26 nM) to **6w** (230 nM). Large electron withdrawing groups are less well tolerated as seen with **14k** (272 nM). Alcohol groups both on the A ring and at the terminal end of the side chain results in a decrease in activity as demonstrated by **14l** and **14m.**

dx.doi.org/10.1021/jm201179h | *J. Med. Chem.* 2012, 55, 1831–1843

Table 8. In Vitro Antimalarial Activities of Structurally More Diverse Bicyclic Quinolones versus 3D7 *P. falciparum*[a]

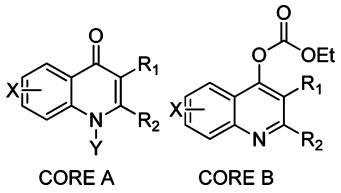

compound	core	X	Y	R^1	R^2	IC_{50} (nM)3D7 ± SD/(IC_{50} (nM) $PfNDH_2$)
20	A	H	H	-Ph*p*CH_2Ph*p*OCF_3	Me	36 ± 6/(492)
22	A	H	H	-Ph*p*OPh*p*OCF_3	Me	10 ± 1.2/(190)
25	A	H	H	-Ph*p*OPh*p*OCF_3	CH_2OH	91 ± 21/(>56 μM)
29	A	H	H	-Ph*p*OPh*p*OCF_3	H	797 ± 130
32a	A	H	H	CO_2Et	-Ph*p*CH_2Ph*p*OCF_3	39.6 ± 6/(268)
32b	A	7-Cl	H	CO_2Et	-Ph*p*CH_2Ph*p*OCF_3	26 ± 1
33a	A	7-Cl	H	CH_2OH	-Ph*p*CH_2Ph*p*OCF_3	63 ± 5
33b	A	7-Cl	H	CH_2OH	-Ph*p*OPh*p*OCF_3	200 ± 22
34a	B	H	H	Me	-Ph*p*CH_2Ph*p*OCF_3	27 ± 4.3
34c	B	H	H	-Ph*p*CH_2Ph*p*OCF_3	Me	27 ± 4.4
34e	B	H	H	Me	-Ph*p*OPh*p*OCF_3	60 ± 12
36a	A	H	OH	Me	-Ph*p*CH_2Ph*p*OCF_3	22 ± 0.4/(55.2)
36b	A	7-Cl	OH	Me	-Ph*p*CH_2Ph*p*OCF_3	149 ± 40
36c	A	H	OH	-Ph*p*CH_2Ph*p*OCF_3	Me	175 ± 80/(13.5)
36d	A	H	OH	H	-Ph*p*CH_2Ph*p*OCF_3	263 ± 64/(71)
36e	A	H	OH	Me	-Ph*p*OPh*p*OCF_3	35 ± 9/(108)
42a	A	H	H	Me	-Ph*p*OPh*p*O$(CH_2)_2$N$(CH_2CH_2)_2$O	>1000
42b	A	H	H	Me	-Ph*p*OPh*m*O$(CH_2)_2$N$(CH_2CH_2)_2$O	719 ± 87
42c	A	H	H	Me	Ph*p*CH_2Ph*m*O$(CH_2)_2$N$(CH_2CH_2)_2$O	355 ± 60/(279)

[a]Numbers in parentheses are IC_{50} (nM) $PfNDH_2$.

Table 8 shows the antimalarial activities of the more structurally diverse bicyclic quinolones. From the small number of 3-aryl compounds synthesized, the effect of altering R^2 can be seen. For this series of compounds Me > CH_2OH > H in terms of antimalarial activity. For a comparison of 3-aryl compounds vs 2-aryl compounds across the full range of in vitro data, see Figure 7. Other comparisons that can be made

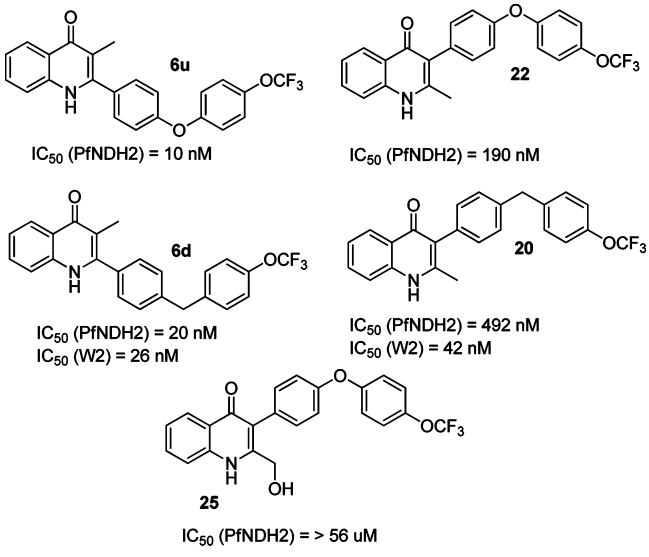

Figure 7. 2-Aryl quinolones vs 3-aryl quinolones.

from the table include the effect of having an ethyl ester at the 3-position. Ester **32a** (39.6 nM) can be compared to its methyl equivalent **6c** (107 nM) and likewise ester **32b** (26 nM) to **6j** (36 nM). In both cases the ester does offer a slightly better activity. The presence of an alcohol at the 3-position does however reduce activity slightly. Core B compounds tested demonstrate good antimalarial activity, but there is no definite trend when compared to their core A counterparts.

The general trend when *N*-hydroxy compounds are compared to the NH variants (**36b** (149 nM) cf **6j** (36 nM), **36c** (175 nM) cf **20** (36 nM), **36d** (263 nM) cf **14e** (48 nM), and **36e** (35 nM) cf **6u** (26 nM)) is a reduction in activity, although **36a** is an exception to this. Generally, the addition of an ethoxy morpholine group leads to a drop in 3D7 activity. This would concur with our previous observations that larger terminal substituents on the side chain are not well tolerated.

Having established the whole cell activity of all quinolone compounds, they were then tested against the PfNDH2 enzyme. Because of the time-consuming nature of the assay[22] and large volume of parasites needed, only a small selection of the most active compounds were then tested against parasite bc_1 in order to establish the selectivity of the compounds against PfNDH2 (see footnote, Table 7). A large number of the quinolones tested demonstrate nanomolar activity against PfNDH2 and some selectivity against parasite bc_1.

From these compounds a selection was tested against the atovaquone resistant TM90C2B strain of *P. falciparum* (IC_{50} for atovaquone is 12 μM in this strain).

Additionally a more select range of compounds were tested against the chloroquine resistant strain of *P. falciparum*, W2. The SAR trends identified from the 3D7 data largely hold true for the W2 data with the presence of a 7-methoxy (**6o**, 13 nM) and 7-Cl (**6j**, 17 nM) groups enhancing activity when compared to unsubstituted **6d** (26 nM).

dx.doi.org/10.1021/jm201179h | *J. Med. Chem.* 2012, 55, 1831−1843

Table 9. In Vitro Antimalarial Activities of Selected Quinolones versus TM90C2B

compound	IC_{50} (nM) TM90C2B ± SD/(IC_{50} (nM) 3D7 ± SD)	compound	IC_{50} (nM) TM90C2B ± SD (IC_{50} (nM) 3D7 ± SD)
6c	416 ± 74 (107 ± 14)	**14e**	251 ± 22 (48 ± 7)
6d	122 ± 26 (117 ± 27)	**14f**	626 ± 69 (16 ± 4)
6e	65 ± 11(26 ± 2)	**15c**	328 ± 48 (19 ± 6)
6f	273 ± 35 (83 ± 9)	**32a**	1400 ± 57 (39.6 ± 6)
6g	577 ± 43 (37 ± 7)	**32b**	92 ± 2 (26 ± 1)
6j	178 ± 9 (36 ± 5)	**33a**	330 ± 58 (63 ± 5)
6q	31 ± 7 (8.4 ± 0.4)	**34a**	6.8 ± 3.5 (27 ± 4.3)
6r	94 ± 3 (34 ± 6)	**34c**	224 ± 47 (27 ± 4.4)
6s	552 ± 35 (105 ± 15)	**34e**	406 ± 74 (60 ± 12)
6u	92 ± 2 (26 ± 1)	**36a**	217 ± 18 (2.2 ± 0.4)
6v	274 ± 58 (73 ± 19)	**36b**	>1000 (149 ± 40)
6w	797 ± 34 (230 ± 43)	**36c**	670 ± 24 (175 ± 80)
11e	1880 ± 150 (407 ± 30)	**36d**	403 ± 38 (263 ± 64)
11f	191 ± 35 (69 ± 11)	**36e**	566 ± 35 (35 ± 9)
11g	207 ± 43 (24 ± 6)		

Table 10. In Vitro Antimalarial Activities of Selected Quinolones versus W2

compound	IC_{50} (nM) W2 ± SD/(IC_{50} (nM) 3D7 ± SD)	compound	IC_{50} (nM) W2 ± SD (IC_{50} (nM) 3D7 ± SD)
6d	26 ± 1.2 (117 ± 27)	**15c**	22 ± 2.5 (19 ± 6)
6j	17 ± 0.6 (36 ± 5)	**20**	42 ± 1.3 (36 ± 6)
6o	13 ± 0.9 (8 ± 2)	**22**	34 ± 3.4 (10 ± 1.2)
14e	36 ± 0.5 (48 ± 7)	**36a**	8 ± 0.7 (22 ± 0.4)

Table 11. In Vivo Peters' Standard 4 Day Test[a]

	% parasite clearance on day 4 (20 mg/kg po)		
	vehicle		
compound	SSV	DET	Na_2CO_3
atovaquone	100	100	ND
6d	100	100	ND
6j	59	100	ND
6u	100	95.4	ND
44	ND	ND	100
45	ND	ND	100

[a]Day 4 suppressive activity of key compounds in male CD-1 mice infected with *Plasmodium berghei*. Mice were exposed to the infection via intraperitoneal injection and then orally dosed with the relevant compound. Data were obtained from 5 mice per group.

A direct comparison of 3-aryl and 2-aryl quinolones can be made from the two pairs of compounds depicted in Figure 7. This clearly depicts a loss of PfNDH2 activity when moving from 2-aryl to 3-aryl examples with **6u** having PfNDH2 activity of 10 nM and its 3-aryl counterpart **22** having activity of 190 nM. **6d** has 20 nM PfNDH2 activity with this droping to 492 nM for 3-aryl quinolone **20**. The most extreme example of this being 3-aryl quinolone **25** which shows no PfNDH2. This trend is also observed with the W2 *P. falciparum* data. All analogues depicted in Figure 7 demonstrate good levels of 3D7 antiparasitic activity.

A selection of the most active quinolones were tested for in vivo activity using Peters' Standard 4-day test (Table 11).[23] Some solubility problems were encountered with the use of SSV (in most cases compounds had to be dosed as suspensions), but the use of DET (compounds fully dissolved) is proof of concept that **6j** (CK-2-68) clears the parasite in vivo with 100% parasite kill being achieved at 20 mg/kg. The pro-drug of **6j**, compound **44** was successfully dosed in a sodium carbonate solution and 100% parasite kill was also seen at 20 mg/kg. **6d** was also potent by oral route in the mouse model with 100% clearance at 20 mg/kg in this model. In the cases where parasite clearance did not reach 100%, we believe this to be a solubility issue as from the table it is clearly vehicle dependent.

Because of **6j** having excellent in vitro activity and selectivity against PfNDH2, it was selected as the lead compound for further investigation.

Cytotoxicity. No significant cytotoxicity was observed for **6j** at any concentration (CC_{50} > 50 μM) in HEPG2 cells. Cytotoxicity data established a selectivity index (CC_{50}/IC_{50}) > 1388.

Human Liver Microsomal Incubations. **6j** was incubated at a concentration of 1 μM with human liver microsomes (1 mg/mL) in the presence of NADPH for 0, 10, 30, and 60 min. After 60 min, 80% of **6j** remained. The in vitro half-life for **6j** was shown to be 226 min, with an intrinsic clearance value of 0.76 mL/min/kg.

CONCLUSIONS

To conclude, a 4−6 step synthesis of a range of bisaryl quinolones with potent antimalarial activity both in vitro and in vivo has been reported. Several compounds within this series have been proven to be selectively active against the PfNDH2 enzyme. Lead compounds within this series have antimalarial activity against the 3D7 strain of *P. falciparum* and PfNDH2 activity in the low nanomolar region and for the most selective quinolone, **6j**, a PfNDH2/Pfbc_1 selectivity ratio of up to 600-fold. It is important to note that additional quinolones in this series have the ability to inhibit both PfNDH2 and bc_1 in the low nanomolar range and this dual targeting of two key mitochondrial enzyme targets may prove to be an advantage over single-targeting inhibitors with respect to drug efficacy and delaying the onset of parasite drug resistance.

Representative quinolones and their phosphate pro-drugs also have proven to be effective at clearing parasitic infection at 20 mg/kg in a murine model of malaria, and further work is in progress to optimize the solubility and ADMET properties of this series.

EXPERIMENTAL SECTION

Chemistry. All reactions that employed moisture sensitive reagents were performed in dry solvent under an atmosphere of nitrogen in oven-dried glassware. All reagents were purchased from Sigma Aldrich

dx.doi.org/10.1021/jm201179h | J. Med. Chem. 2012, 55, 1831−1843

or Alfa Aesar chemical companies, and were used without purification. Thin layer chromatography (TLC) was carried out on Merck silica gel 60 F-254 plates and UV inactive compounds were visualized using iodine or anisaldehyde solution. Flash column chromatography was performed on ICN Ecochrom 60 (32−63 mesh) silica gel eluting with various solvent mixtures and using an air line to apply pressure. NMR spectra were recorded on a Bruker AMX 400 (^{1}H, 400 MHz; ^{13}C, 100 MHz) spectrometer. Chemical shifts are described in parts per million (δ) downfield from an internal standard of trimethylsilane. Mass spectra were recorded on a VG analytical 7070E machine and Fisons TRIO spectrometer using electron ionization (EI) and chemical ionization (CI). All compounds were found to be >95% pure by HPLC unless specified below. See Supporting Information for experimental and data on all intermediates.

General Procedure for the Synthesis of Quinolones 6. The appropriately substituted oxazoline **5** (4 mmol, 1.0 equiv) was added to a solution of ketone **3** (4 mmol, 1.0 equiv) and *para*-toluenesulfonic acid (20 mol %) in *n*-butanol (10 mL). The reaction mixture was heated to 130 °C under nitrogen and stirred for 24 h. The solvent was removed under a vacuum and water (20 mL) was added. The aqueous solution was extracted with EtOAc (3 × 20 mL), dried over $MgSO_4$, and concentrated under a vacuum. The product was purified by column chromatography (eluting with 20−80% EtOAc in *n*-hexane) to give quinolone **6**.

6d: White powder (Yield 36%); mp 212−214 °C; ^{1}H NMR (400 MHz, DMSO) δ_H 8.98 (s, 1H, NH), 8.27 (d, J = 8.3 Hz, 1H), 7.60 (d, J = 8.1 Hz, 1H), 7.56 (dt, J = 1.4 Hz, 8.3 Hz, 1H), 7.9 (d, J = 8.1 Hz, 2H), 7.26 (dt, J = 1.5 Hz, 8.1 Hz, 1H), 7.20 (d, J = 8.0 Hz, 2H), 7.16 (d, J = 8.6 Hz, 2H), 7.11 (d, J = 8.1 Hz, 2H), 3.96 (s, 2H), 2.01 (s, 3H); ^{13}C NMR (100 MHz, DMSO), δ_C 178.7, 149.0, 142.4, 139.5, 133.8, 132.0, 130.6, 129.4, 126.4, 123.8, 121.5, 118.0, 116.6, 41.3, 12.9; MS (ES$^+$), $[M + H]^+$ m/z 410.1, HRMS calculated for 410.1368 $C_{24}H_{19}NO_2F_3$, found 410.1348.

6j: White solid (Yield 30%); mp 240−242 °C; ^{1}H NMR (400 MHz, MeOD) δ 8.27 (d, J = 8.8 Hz, 1H), 7.62 (s, 1H), 7.52−7.45 (m, 5H), 7.43−7.34 (m, 3H), 7.24 (d, J = 7.9 Hz, 1H), 4.15 (s, 2H), 2.05 (s, 3H); MS (ES$^+$) m/z 444 $[M + H]^+$ Acc mass found: 444.0962, calculated 444.0978 for $C_{24}H_{18}NO_2F_3Cl$.

6u: White solid (Yield 28%); mp 207−208 °C; ^{1}H NMR (400 MHz, $CDCl_3$) δ 8.24 (d, J = 8.2 Hz, 1H), 7.61 (d, J = 8.3 Hz, 1H), 7.54 (t, J = 7.5 Hz, 1H), 7.42 (d, J = 8.5 Hz, 2H), 7.31 − 7.17 (m, 3H), 7.03 (dd, J = 8.6, 6.9 Hz, 4H), 2.02 (s, 3H); ^{13}C NMR (100 MHz, $CDCl_3$) δ 179.14, 158.36, 155.06, 148.33, 145.44, 139.67, 131.94, 130.92, 130.58, 125.83, 123.79, 123.76, 123.15, 120.76, 118.57, 118.17, 116.35, 12.76; MS (ES$^+$) m/z 412 $[M + H]^+$ Acc mass found: 412.1175, calculated 412.1161 for $C_{23}H_{17}NO_3F_3$.

Procedure for the Synthesis of Phosphate Pro-Drug 44. A suspension of phosphate **43** (0.18 mmol, 1.0 equiv) in anhydrous methanol (10 mL) was subjected to hydrogenation in the presence of 10% Pd/C (50 mg) at room temperature for 10 min. The catalysts and any precipitates were filtered off and the methanol portion was analyzed by TLC. The solvent was removed in vacuo to give the desired phosphate pro-drug **44** and no further purification was required. White solid (Yield 80%); mp 201−203 °C; ^{1}H NMR (400 MHz, $CDCl_3$) δ 11.82 (s, 1H), 11.62 (s, 1H), 8.32 (d, J = 8.2 Hz, 1H), 8.26 (d, J = 8.0 Hz, 1H), 8.12 (d, J = 8.4 Hz, 1H), 8.06 (s, 1H), 7.91 (t, J = 8.2 Hz, 1H), 7.82 (t, J = 8.1 Hz, 1H), 7.68 (d, J = 8.0 Hz, 1H), 7.56 (d, J = 8.2 Hz, 2H), 7.52 (d, J = 8.0 Hz, 2H), 7.46−7.32 (m, 12H), 4.12 (s, 2H), 4.09 (s, 2H), 2.40 (s, 3H), 2.37 (s, 3H). ^{31}P NMR (162 MHz, $CDCl_3$) δ −5.027, −5.396; MS (ES$^-$) m/z 522 $[M - H]^-$ Acc mass found: 522.0471, calculated 522.0485 for $C_{24}H_{17}NO_5F_3PCl$.

Procedure for the Synthesis of Morpholine Pro-Drug 45. Quinolone **6j** (0.31 mmol) in anhydrous THF was added ^{t}BuOK (52.7 mg, 0.47 mmol) at room temperature. The mixture was stirred for 1/2 h. 4-Morpholinecarbonyl chloride (0.05 mL, 0.41 mmol) was added. The mixture was stirred for a further 2 h (followed by TLC). The reaction was quenched with brine and was extracted with ethyl acetate, dried over Na_2SO_4, filtered, and concentrated to an oil. The crude product was purified by column chromatography using 20% ethyl acetate in hexane to give 43 as a white solid (Yield 66%); mp 148−150 °C; ^{1}H NMR (400 MHz, $CDCl_3$) δ 8.12 (s, 1H), 7.74 (d, J = 8.9 Hz, 1H), 7.53 (d, J = 8.1 Hz, 2H), 7.49 (d, J = 8.9 Hz, 1H), 7.30 (d, J = 8.1 Hz, 2H), 7.24 (d, J = 8.9 Hz, 2H), 7.14 (d, J = 8.8 Hz, 2H), 4.06 (s, 2H), 3.87−3.83 (m, 6H), 3.65 (brs, 2H), 2.30 (s, 3H); MS (ES$^+$) m/z 557 $(M + H)^+$ Acc mass found: 557.1443, calculated 557.1455 for $C_{29}H_{25}N_2O_4F_3Cl$.

Biology. *Parasite Culture.* *Plasmodium* blood stage cultures[24] and drug sensitivity[25] were determined by established methods. IC_{50}s (50% inhibitory concentrations) were calculated by using the four-parameter logistic method (Grafit program; Erithacus Software, United Kingdom)

High-Throughput Screening (HTS). PfNDH2 activity was measured using an end-point assay in a 384-well plate format. Final assay concentrations used were 200 μM NADH, 10 mM KCN, 1 μg/mL F571 membrane,[6] and 20 μM decylubiquinone (dQ). A pre-read at 340 nm was obtained prior to the addition of dQ to initiate the reaction followed by a post-read at 1 min. HDQ was used as positive control at 5 μM. The agreed QC pass criteria was $Z' > 0.6$ and signal/background >10. Compounds were selected by the described chemoinformatics algorithms from the Biofocus DPI compound library (Galapagos Company).

Enzymology. *P. falciparum* cell-free extracts were prepared from erythrocyte-freed parasites as described previously,[22] and recombinant PfNDH2 was prepared from the *Escherichia coli* heterologous expression strain F571.[6] PfNDH2 and bc_1 activities were measured as described previously.[6,22]

Pharmacology. In vivo efficacy studies were measured against *P. berghei* in the standard 4-day test.[23] All in vivo studies were approved by the appropriate institutional animal care and use committee and conducted in accordance with the International Conference on Harmonization (ICH) Safety Guidelines.

■ ASSOCIATED CONTENT

Ⓢ Supporting Information

(1) Additional figures. (2) Experimental details for all intermediates. (3) Further details on chemoinformatics. (4) Melting point − torsion angle analysis. This material is available free of charge via the Internet at http://pubs.acs.org.

■ AUTHOR INFORMATION

Corresponding Author

*(N.B.) Tel: 0151 794 3877 Fax: 0151 794 3588. E-mail: ngberry@liv.ac.uk. (G.A.B.) Tel:0151-705-3151. E-mail: biagini@liverpool.ac.uk. (S.A.W.) Tel: 0151-705-2568. E-mail: saward@liverpool.ac.uk. (P.M.O.) Tel: 0151-794-3553. E-mail: p.m.oneill01@liv.ac.uk.

■ ACKNOWLEDGMENTS

We thank Professor Dennis Kyle (College of Public Health, University of South Florida) for supplying the atovaquone resistant isolate TM90C2B (Thailand) and Dr. Jiri Gut and Professor Phil Rosenthal for the W2 data in Table 10 (Department of Medicine, University of California, San Francisco, USA). We also thank the staff and patients of Ward 7Y and the Gastroenterology Unit, Royal Liverpool Hospital, for their generous donation of blood. This work was supported by grants from the Leverhulme Trust, the Wellcome Trust (Seeding Drug Discovery Initiative), and the National Institute of Health Research (NIHR, BRC Liverpool).

■ ABBREVIATIONS

SAR, structure−activity relationship; NADH, nicotinamide adenine dinucleotide; bc_1, ubihydroquinone; ADMET, absorption, distribution, metabolism, excretion, toxicity; HTS, high throughput screen; PTSA, *para*-toluene sulfonic acid; LAH,

lithium aluminum hydride; DMF, dimethylformamide; *m*-CPBA, *meta*-chloro per benzoic acid; KOH, potassium hydroxide; THF, tetrahydrofuran; DCM, dichloromethane; NADPH, nicotinamide adenine dinucleotide phosphate; NMP, *N*-methyl-2-pyrrolidone; SSV, standard suspension vehicle; DET, 5% DMSO and 5% EtOH in tetraglycol

REFERENCES

(1) (a) Snow, R. W.; Trape, J. F.; Marsh, K. The past, present and future of childhood malaria mortality in Africa. *Trends Parasitol.* **2001**, *17* (12), 593−597. (b) White, N. J. Antimalarial drug resistance. *J. Clin. Invest.* **2004**, *113* (8), 1084−1092.

(2) *Malaria*; Fact Sheet Number 94; World Health Organization: Geneva, Switzerland, 2009.

(3) (a) Burrows, J. N.; Chibale, K.; Wells, T. N. The state of the art in anti-malarial drug discovery and development. *Curr. Top. Med. Chem.* **2011**, *11* (10), 1226−1254. (b) A research agenda for malaria eradication: drugs. *PLoS Med.* **2011**, *8* (1), e1000402.

(4) (a) Biagini, G. A.; Viriyavejakul, P.; O'Neill, P, M.; Bray, P. G.; Ward, S. A. Functional characterization and target validation of alternative complex I of *Plasmodium falciparum* mitochondria. *Antimicrob. Agents Chemother.* **2006**, *50* (5), 1841−1851. (b) Fisher, N.; Bray, P. G.; Ward, S. A.; Biagini, G. A. The malaria parasite type II NADH:quinone oxidoreductase: an alternative enzyme for an alternative lifestyle. *Trends Parasitol.* **2007**, *23* (7), 305−310.

(5) Fry, M.; Pudney, M. Site of action of the antimalarial hydroxynaphthoquinone, 2-[trans-4- (4′-chlorophenyl) cyclohexyl]-3-hydroxy-1,4-naphthoquinone (566C80). *Biochem. Pharmacol.* **1992**, *43* (7), 1545−1553.

(6) Fisher, N.; Warman, A. J.; Ward, S. A.; Biagini, G. A. Chapter 17 Type II NADH: quinone oxidoreductases of *Plasmodium falciparum* and Mycobacterium tuberculosis kinetic and high-throughput assays. *Methods Enzymol.* **2009**, *456*, 303−320.

(7) (a) Durant, J. L.; Leland, B. A.; Henry, D. R.; Nourse, J. G. Reoptimization of MDL keys for use in drug discovery. *J. Chem. Inf. Comput. Sci.* **2002**, *42* (6), 1273−1280. (b) Rogers, D.; Hahn, M. Extended-connectivity fingerprints. *J. Chem. Inf. Model.* **2010**, *50* (5), 742−754.

(8) Willett, P. Similarity-based virtual screening using 2D fingerprints. *Drug Discovery Today* **2006**, *11* (23−24), 1046−1053.

(9) Geppert, H.; Vogt, M.; Bajorath, J. Current trends in ligand-based virtual screening: molecular representations, data mining methods, new application areas, and performance evaluation. *J. Chem. Inf. Model.* **2010**, *50* (2), 205−216.

(10) Liu, K.; Feng, J.; Young, S. S. PowerMV: A software environment for molecular viewing, descriptor generation, data analysis and hit evaluation. *J. Chem. Inf. Model.* **2005**, *45* (2), 515−522.

(11) (a) Lipinski, C. A. Drug-like properties and the causes of poor solubility and poor permeability. *J. Pharmacol. Toxicol. Methods* **2000**, *44* (1), 235−249. (b) Waring, M. J. Lipophilicity in drug discovery. *Exp. Opin. Drug Discovery* **2010**, *5* (3), 235−248. (c) Hughes, J. D.; Blagg, J.; Price, D. A.; Bailey, S.; DeCrescenzo, G. A.; Devraj, R. V.; Ellsworth, E.; Fobian, Y. M.; Gibbs, M. E.; Gilles, R. W.; Greene, N.; Huang, E.; Krieger-Burke, T.; Loesel, J.; Wager, T.; Whiteley, L.; Zhang, Y. Physiochemical drug properties associated with in vivo toxicological outcomes. *Bioorg. Med. Chem. Lett.* **2008**, *18* (17), 4872−4875. (d) Gleeson, M. P. Generation of a set of simple, interpretable ADMET rules of thumb. *J. Med. Chem.* **2008**, *51* (4), 817−834. (e) Veber, D. F.; Johnson, S. R.; Cheng, H. Y.; Smith, B. R.; Ward, K. W.; Kopple, K. D. Molecular properties that influence the oral bioavailability of drug candidates. *J. Med. Chem.* **2002**, *45* (12), 2615−2623.

(12) (a) Fray, M. J.; Bull, D. J.; Carr, C. L.; Gautier, E. C.; Mowbray, C. E.; Stobie, A. Structure-activity relationships of 1,4-dihydro-(1H,4H)-quinoxaline-2,3-diones as *N*-methyl-D-aspartate (glycine site) receptor antagonists. 1. Heterocyclic substituted 5-alkyl derivatives. *J. Med. Chem.* **2001**, *44* (12), 1951−1962. (b) Ishikawa, M.; Hashimoto, Y. Improvement in aqueous solubility in small molecule drug discovery programs by disruption of molecular planarity and symmetry. *J. Med. Chem.* **2011**, *54*, 1539−1554.

(13) Yalkowsky, S. H.; Banerjee, S. *Aqueous Solubility: Methods of Estimation for Organic Compounds*; Marcel Dekker: New York, 1992.

(14) Luo, F.-T.; Ravi, V. K.; Xue, C. The novel reaction of ketones with o-oxazoline-substituted anilines. *Tetrahedron* **2006**, *62*, 9365−9372.

(15) Bueno, J. M.; Manzano, P.; García, M.; J., C.; Puente, M.; Lorenzo, A.; García, A.; Ferrer, S.; Gómez, R. M.; Fraile, M. T.; Lavander, J. L.; Fiandor, J. M.; Vidala, J.; Herreros, E.; Gargallo-Violaa, D. Potent Antimalarial 4-pyridones with improved physico-chemical properties. *Bioorg. Med. Chem. Lett.* **2011**, *21*, 5214−5218.

(16) Bueno-Calderon, J. M.; Fiandor-Roman, J. M.; Puente-Felipe, M.; Chicharrp-Gonzalo, J.; Kusalakumari Sukamar, S. K.; Maleki, M., Phosphate ester of a 4-pyridone derivative and its use in the chemotherapy of parasitic infections. WO2010094738, 26th August 2010.

(17) Cundy, K. C.; Annamalai, T.; Bu, L.; De Vera, J.; Estrela, J.; Luo, W.; Shirsat, P.; Torneros, A.; Yao, F.; Zou, J.; Barrett, R. W.; Gallop, M. A. XP13512 [(±)-1-([(alpha-isobutanoyloxyethoxy)carbonyl] aminomethyl)-1-cyclohexane acetic acid], a novel gabapentin prodrug: II. Improved oral bioavailability, dose proportionality, and colonic absorption compared with gabapentin in rats and monkeys. *J. Pharmacol. Exp. Ther.* **2004**, *311* (1), 324−333.

(18) (a) Hofle, G.; Bohlendorf, B.; Fecker, T.; Sasse, F.; Kunze, B. Semisynthesis and antiplasmodial activity of the quinoline alkaloid aurachin E. *J. Nat. Prod.* **2008**, *71* (11), 1967−1969. (b) Miyoshi, H.; Takegami, K.; Sakamoto, K.; Mogi, T.; Iwamura, H. Characterization of the ubiquinol oxidation sites in cytochromes bo and bd from Escherichia coli using aurachin C analogues. *J. Biochem.* **1999**, *125* (1), 138−142. (c) Lin, S. S.; Gross, U.; Bohne, W. Type II NADH dehydrogenase inhibitor 1-hydroxy-2-dodecyl-4(1H)quinolone leads to collapse of mitochondrial inner-membrane potential and ATP depletion in Toxoplasma gondii. *Eukaryotic Cell* **2009**, *8* (6), 877−887. (d) Dong, C. K.; Patel, V.; Yang, J. C.; Dvorin, J. D.; Duraisingh, M. T.; Clardy, J.; Wirth, D. F. Type II NADH dehydrogenase of the respiratory chain of *Plasmodium falciparum* and its inhibitors. *Bioorg. Med. Chem. Lett.* **2009**, *19* (3), 972−975.

(19) Woschek, A.; Mahout, M.; Mereiter, K.; Hammerschmidt, F. Synthesis of 2-heptyl-1-hydroxy-4(1H)-quinolone - unexpected rearrangement of 4-(Alkoxycarbonyl)quinoline N-oxides to 1-(Alkoxycarbonyloxy)-4(1H)-quinolones. *Synthesis* **2007**, *10*, 1517−1522.

(20) Zask, A.; Kaplan, J.; Verheijen, J. C.; Richard, D. J.; Curran, K.; Brooijmans, N.; Bennett, E. M.; Toral-Barza, L.; Hollander, I.; Ayral-Kaloustian, S.; Yu, K. Morpholine derivatives greatly enhance the selectivity of mammalian target of rapamycin (mTOR) inhibitors. *J. Med. Chem.* **2009**, *52* (24), 7942−7945.

(21) Chou, L. C.; Chen, C. T.; Lee, J. C.; Way, T. D.; Huang, C. H.; Huang, S. M.; Teng, C. M.; Yamori, T.; Wu, T. S.; Sun, C. M.; Chien, D. S.; Qian, K.; Morris-Natschke, S. L.; Lee, K. H.; Huang, L. J.; Kuo, S. C. Synthesis and preclinical evaluations of 2-(2-fluorophenyl)-6,7-methylenedioxyquinolin-4-one monosodium phosphate (CHM-1-P-Na) as a potent antitumor agent. *J. Med. Chem.* **2010**, *53* (4), 1616−1626.

(22) Biagini, G. A.; Fisher, N.; Berry, N.; Stocks, P. A.; Meunier, B.; Williams, D. P.; Bonar-Law, R.; Bray, P. G.; Owen, A.; O'Neill, P. M.; Ward, S. A. Acridinediones: selective and potent inhibitors of the malaria parasite mitochondrial bc1 complex. *Mol. Pharmacol.* **2008**, *73* (5), 1347−1355.

(23) Peters, W.; Robinson, B. L. *Malaria*; Academic Press: San Diego, 1999.

(24) Trager, W.; Jensen, J. B. Human malaria parasites in continuous culture. *Science* **1976**, *193* (4254), 673−675.

(25) Smilkstein, M.; Sriwilaijaroen, N.; Kelly, J. X.; Wilairat, P.; Riscoe, M. Simple and inexpensive fluorescence-based technique for high-throughput antimalarial drug screening. *Antimicrob. Agents Chemother.* **2004**, *48* (5), 1803−1806.